Electronic Supplementary Information

Fascinating the Supercapacitive Performance of Activated Carbon Electrodes with Enhanced Energy Density in Multifarious Electrolytes

M. Karnan[a,b], AG Karthick Raj[a], K. Subramani[a] , S. Santhoshkumar[a], and

M. Sathish[a,b]*

[a]Functional Materials Division, CSIR-Central Electrochemical Research Institute,
Karaikudi – 630 003, Tamilnadu, India
[b]Academy of Scientific and Innovative Research (AcSIR),
Ghaziabad-201 002, India

Corresponding authors: *marappan.sathish@gmail.com*; *msathish@cecri.res.in*

Table ST1: A detailed literature reports for the bio-derived activated carbon-based supercapacitors with various electrolytes

Material	Electrolyte	Capacitance	Current Density	Energy Density (Wh/Kg)	Power Density(W/Kg)	Year	Reference
Carbon derived from pomelo peel	KOH	342	1	47.5		2012	1
Activated carbon	KNO_3	128	1	10.4	382	2015	2
Porous grapheme carbon from cellulose	KOH	280	1	-	-	2015	3
carbon from sewage sludge	KOH	379	0.5			2015	4
carbon from white poplar	KOH	370	0.1	8.6	5000	2016	5
Tamarind fruit shell	PVA/H_2SO_4	412	1.56	9.16	-	2013	6
Nitrogen-Doped Carbon Nanosheets	H_2SO_4	106	2	5.92	1000	2017	7
Soybean Root-Derived Hierarchical Porous Carbon	KOH	276	0.5	9.5	-	2016	8
Sulfur doped carbon from ginkgo leCLes	6M KOH	364	0.5	-	-	2017	9
Carbon derived from Lotus stems	KOH	360.5	0.5	40.55	-	2018	10

Material	Electrolyte	Capacitance (F/g)	Current Density (A/g)	Energy Density (Wh/Kg)	Power Density (Kw/Kg)	Year	Reference
Porous graphene carbon from cellulose	[EMIM][BF_4]	196	1	83.5		2015	[3]
Soybean Root-Derived Hierarchical Porous Carbon	[EMIM][BF_4]	239	5	100.5	63	2016	[8]
Carbon	Imidazolium -based ionic liquid crystal	131.43	0.37	33.79	1.033	2016	[11]
Graphene oxide	[EMIM][BF_4]	271		13.3		2016	[12]
Reduced Graphene oxide	BMP-DCA	764.53	1	245	6.526	2016	[13]
Sulfur doped carbon from ginkgo leCLes	[EMIM][BF_4]	202	0.5	16	50	2017	[9]
Carbon Nanofiber	1-ethyl-3-methylimidazolium bis(trifluoromethylsulfonyl)imide	153	1	65		2017	[14]
Carbon derived from pine tree saw dust	[EMIM][BF_4]	224	0.1	92		2017	[15]

Materials	Electrolyte	Capacitance (F/g)	Current Density (A/g)	Energy Density (Wh/Kg)	Power Density (Kw/Kg)	Year	Reference
Carbon derived from watermelon rind	EMIM TFSI	313	1	174	20	2018	[16]
Carbon derived from silkworm cocoon	[EMIM][BF_4]	263.5	0.5	112.1	23.91	2018	[17]
Carbon derived from Corn stalk	NEt4BF4-PC	47.3	1	61.3	10.5	2013	[18]
Meso porous carbon from rice husk and peanut shell	Et_4NBF_4/PC	200	0.05	19.3	1.007	2013	[19]
Porous grapheme carbon from cellulose	TEABF4/AN	171	2			2015	[3]
KOH-activated carbon from natural lignin	tetraethylammoniumtetrafluoroborate	87	1.5			2014	[20]
Carbon bead – self emulsifying novolacethanol-water system	1M tetraethylammoniumtetrafluoroborate in propylene carbonate	123				2016	[21]
Carbon derived from pine tree saw dust	$TEABF_4$/AN	146	0.1	26		2017	[15]

Materials	Electrolyte	Capacitance (F/g)	Current Density (A/g)	Energy Density (Wh/Kg)	Power Density (Kw/Kg)	Year	Reference
Carbon derived from silkworm cocoon	1.0M $TEABF_4$/AN	156.1	5			2018	[17]

Aqueous Electrolyte Organic Electrolyte Ionic Electrolyte Redox Additive Electrolyte

Carbon Source	Electrolyte	Redox Additive	Specific surface area	Capacitance	Current Density	Power Density	Energy Density	Reference
2D Carbon nanosheets	H_2SO_4	1, 4-dihydroxyanthraquinone(DQ) And hydroquinone(HQ)	1052 $m^2 g^{-1}$	239 Fg^{-1}	3 Ag^{-1}	500 Wkg^{-1}	21.1 Wh kg^{-1}	[22]
Nanoporus graphitic carbon materials	KOH	4-(4-nitrophenylazo)-1-naphthol (NPN)	1052 $m^2 g^{-1}$	239 Fg^{-1}	5 Ag^{-1}			[23]
Nitrogen doped sheet like carbon	H_2SO_4	4-hydroxybenzoic acid (HBA), 3,4-dihydroxybenzoic acid (DHBA), and 3,4,5-trihydroxybenzoic acid (THBA)	607 $m^2 g^{-1}$	337 Fg^{-1} (DHBA) 166 Fg^{-1} (HBA)	2 Ag^{-1}	1.0 kW kg^{-1}	10.5/14.7 Wh kg^{-1}	[7]
Nano-porus Carbon	H_2SO_4	ferrous ammonium sulfate	2208 $m^2 g^{-1}$	1499 Fg^{-1}	10 Ag^{-1}	4.5 kW kg^{-1}	58.7 Wh kg^{-1}	[24]
PANI	H_2SO_4	Fe^{3+}/Fe^{2+}		1062 Fg^{-1}	2 Ag^{-1}	774.0 W kg^{-1}	22.1 Wh kg^{-1}	[25]
Multiwall carbon nanotubes/ metal oxide composites	1M Li_2SO_4	KI	92 $m^2 g^{-1}$	96 Fg^{-1}	1 Ag^{-1}	950 W kg^{-1}	65 Wh kg^{-1}	[26]
Activated Carbon	$VOSO_4$ & Na_2MoO_4	PVA – H_2SO_4	2167 $m^2 g^{-1}$	543.4 Fg^{-1}	0.5 Ag^{-1}	245 W kg^{-1}	17.9 Wh kg^{-1}	[27]
Carbon black	Anthraquinone-2,7-	KNO_3	1729 $m^2 g^{-1}$	225 Fg^{-1}	1.0 Ag^{-1}	412 W kg^{-1}	21.2 Wh kg^{-1}	[2]

	disulphonate (AQDS)							
Biomass derived porous activated carbon	$VOSO_4$	1 M H_2SO_4	683.26 $m^2 g^{-1}$	630.6 Fg^{-1}	1.0m Ag^{-1}	325 W kg^{-1}	13.7 Wh kg^{-1}	[28]

Aqueous Electrolyte Organic Electrolyte Ionic Electrolyte Redox Additive Electrolyte

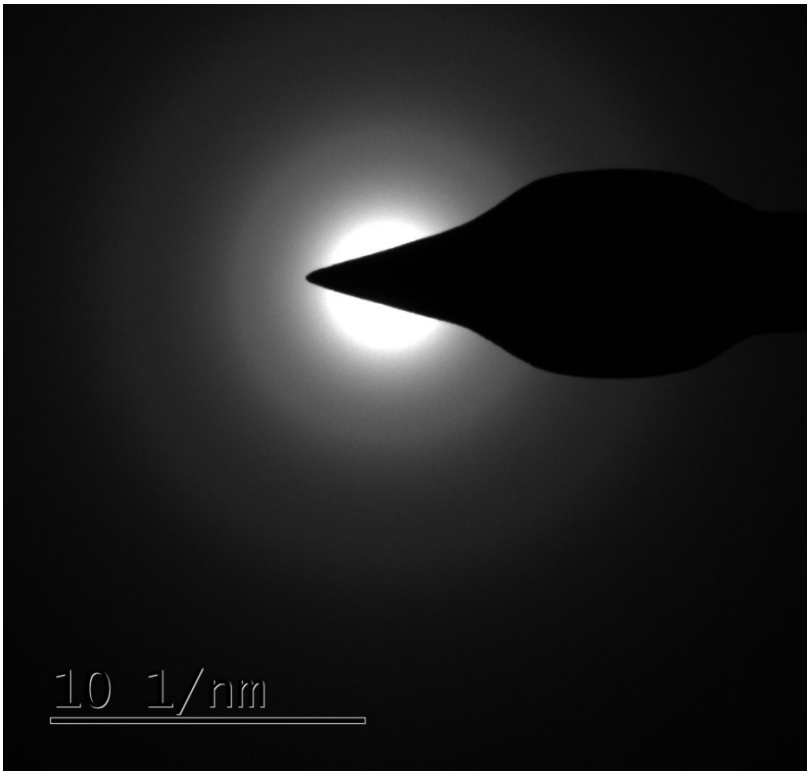

Fig. S1 SAED pattern of CL-700

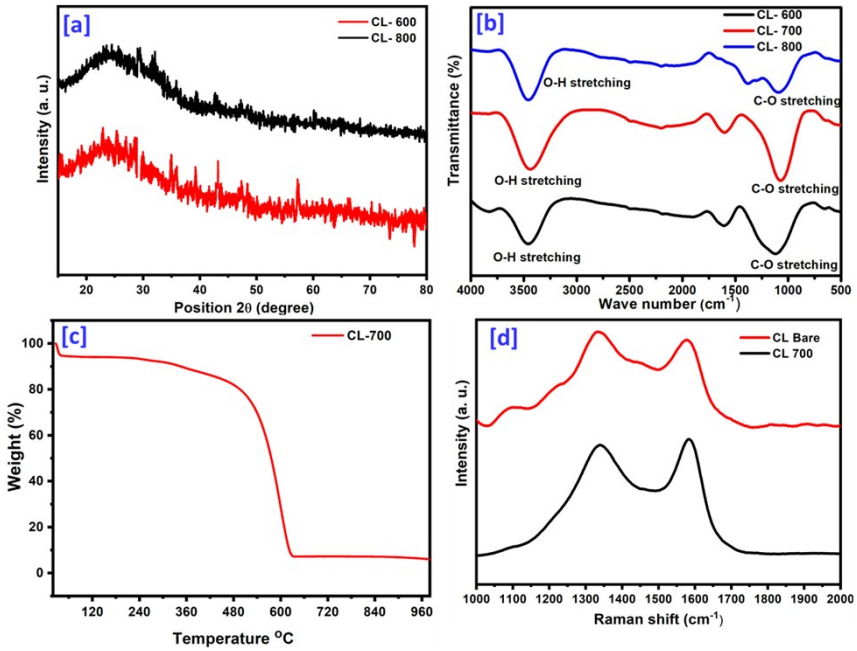

Fig. S2 (a) XRD pattern of CL-600 and CL-800, (b) FT-IR spectrum of all the three activated carbons, (c) TGA plot for CL-700 and (d) Raman spectra for CL- bare and CL-700

Table ST2. CHNS data for CL-600, CL-700 and CL-800 samples.

Material	Carbon (%)	Hydrogen (%)	Nitrogen (%)	Sulphur (%)
CL-600	72.7	2.0354	0.78	0.539
CL-700	78.23	1.654	0.421	0.567
CL-800	79.23	1.987	0.897	0.678

Table ST3. The calculated specific capacitance of CL-600, CL-700 and CL-800 electrode materials at different current densities.

Current rate (A/g)	Specific capacitacne (F/g)		
	CL-600	CL-700	CL-800
1	480	555	365
2	455	546	320
3	380	475	260
4	360	460	223
5	345	454	190
10	290	350	120

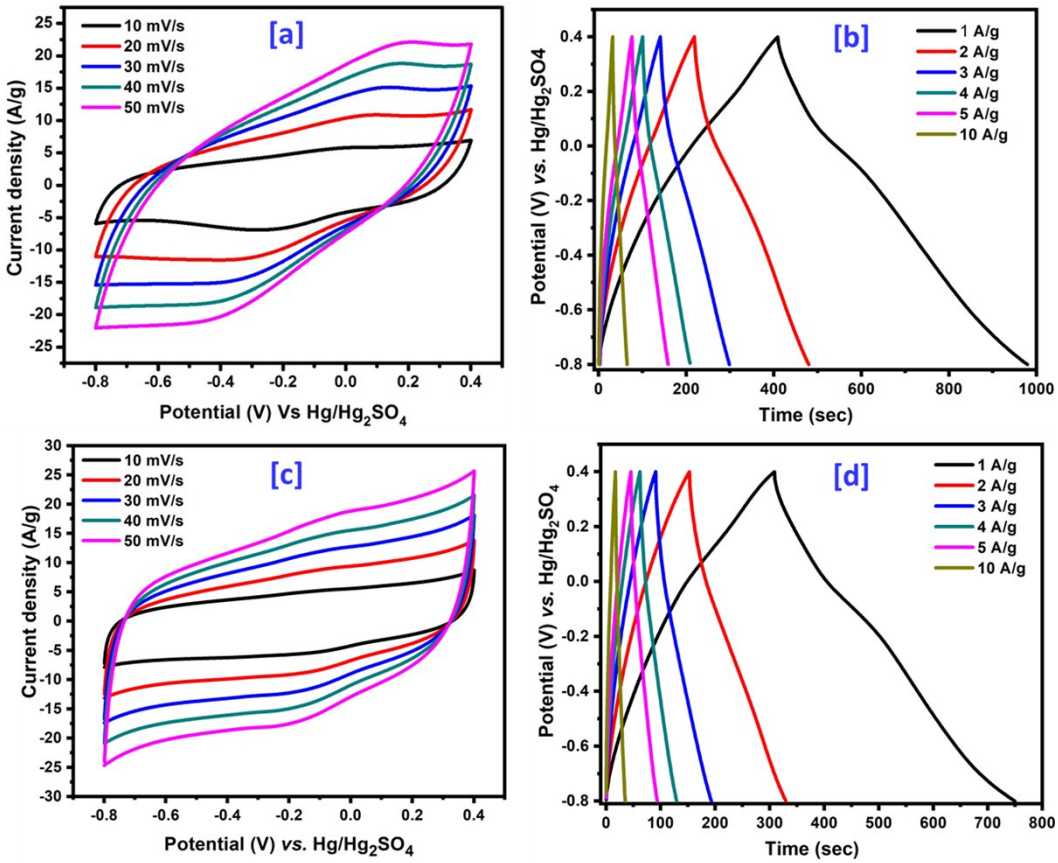

Figure S3. CV and CD profile of (a-b) CL-600 and (c-d) CL- 800.

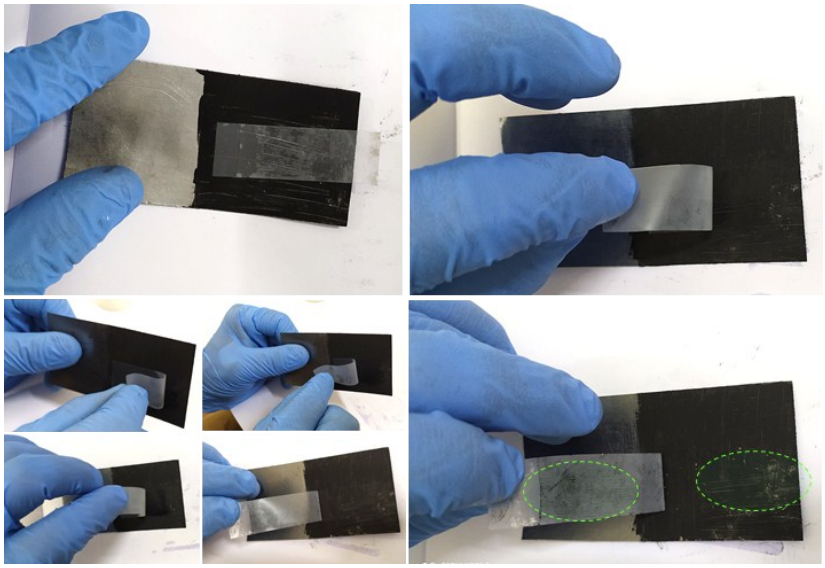

Figure S4. Tape testing for CL-700 electrode material.

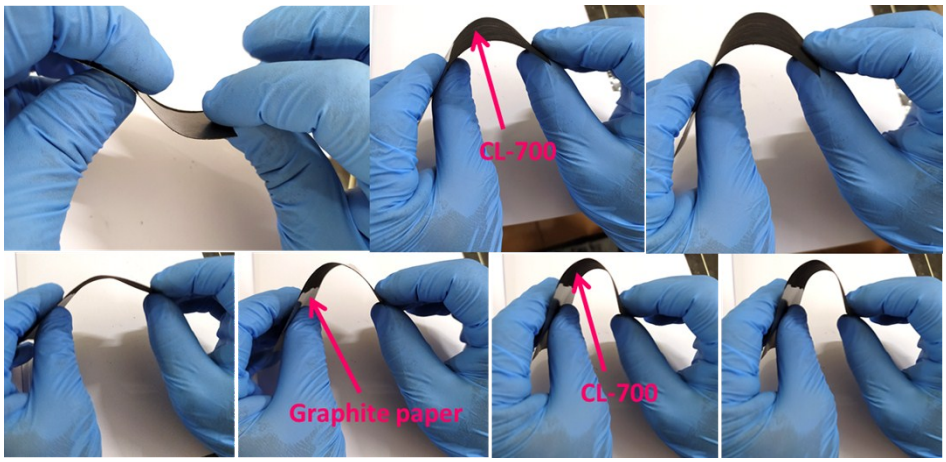

Figure S5. Mechanical stability testing for CL-700 electrode material with different bending angle in both directions.

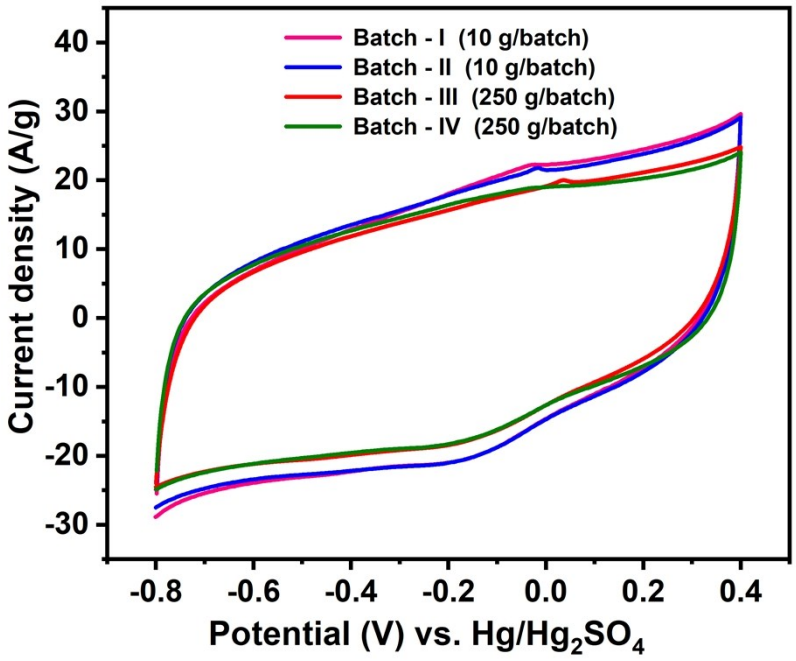

Figure S6. CV profile of CL-700 electrode materials prepared at different batch.

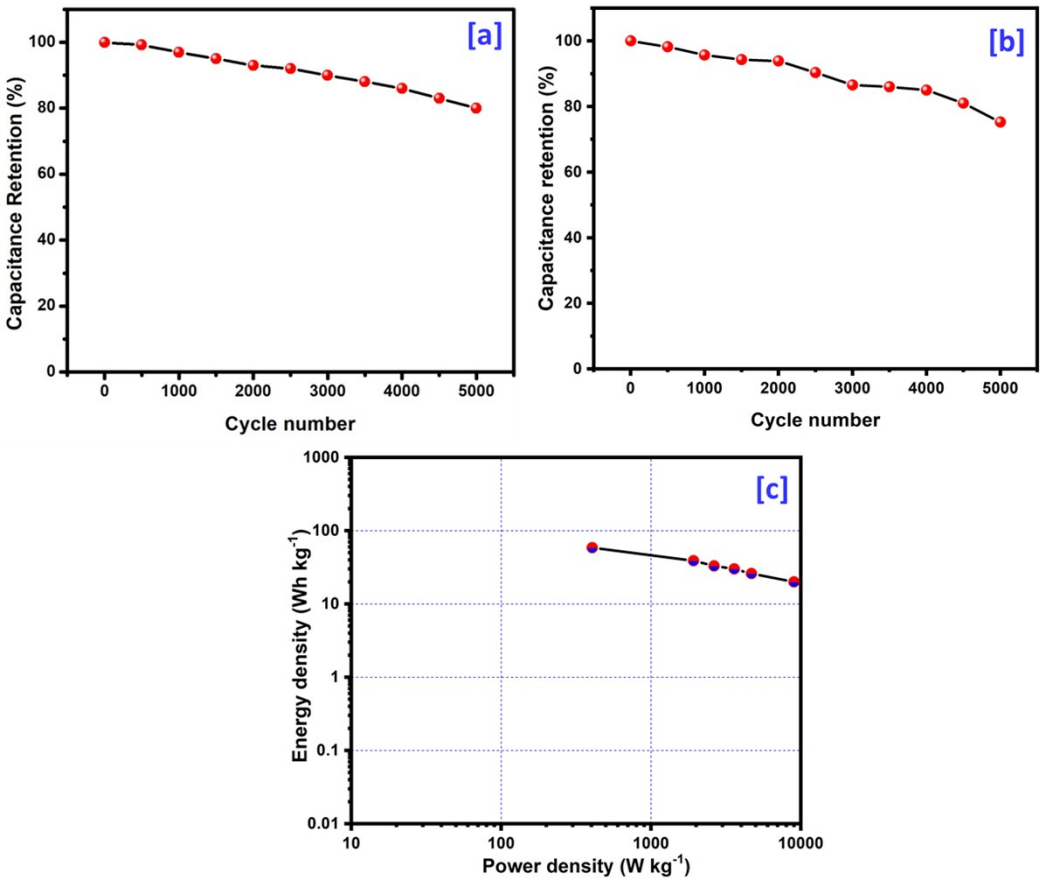

Figure S7. (a) Cyclability profile of CL-700 symmetric three electrode cell for 5000 cycles at 5 A/g current density of CL-700 in 1 M Na_2SO_4 + KI redox additive electrolyte (b) Cyclability profile of CL-700 symmetric two electrode cell for 5000 cycles at 5 A/g current density of CL-700 in 1 M Na_2SO_4 + KI redox additive electrolyte (c) Ragone plot of CL-700 symmetric cell in 1 M Na_2SO_4 + KI redox additive electrolyte.

References

1 C. Peng, J. Lang, S. Xu and X. Wang, *RSC Adv.*, 2014, **4**, 54662–54667.

2 Y. Tian, R. Xue, X. Zhou, Z. Liu and L. Huang, *Electrochim. Acta*, 2015, **152**, 135–139.

3 J. Huang, J. Wang, C. Wang, H. Zhang, C. Lu and J. Wang, *Chem. Mater.*, 2015, **27**, 2107–2113.

4 H. Feng, M. Zheng, H. Dong, Y. Xiao, H. Hu, Z. Sun, C. Long, Y. Cai, X. Zhao, H. Zhang, B. Lei and Y. Liu, *J. Mater. Chem. A*, 2015, **3**, 15225–15234.

5 C. Wang and T. Liu, *RSC Adv.*, 2016, **6**, 105540–105549.

6 S. T. Senthilkumar, R. K. Selvan, J. S. Melo and C. Sanjeeviraja, *ACS Appl. Mater. Interfaces*, 2013, **5**, 10541–10550.

7 W. Hu, D. Xu, X. N. Sun, Z. H. Xiao, X. Y. Chen and Z. J. Zhang, *ACS Sustain. Chem. Eng.*, 2017, **5**, 8630–8640.

8 N. Guo, M. Li, Y. Wang, X. Sun, F. Wang and R. Yang, *ACS Appl. Mater. Interfaces*, 2016, **8**, 33626–33634.

9 E. Hao, W. Liu, S. Liu, Y. Zhang, H. Wang, S. Chen, F. Cheng, S. Zhao and H. Yang, *J. Mater. Chem. A*, 2017, **5**, 2204–2214.

10 S. Yan, J. Lin, P. Liu, Z. Zhao, J. Lian, W. Chang, L. Yao, Y. Liu, H. Lin and S. Han, *RSC Adv.*, 2018, **8**, 6806–6813.

11 R. Sasi, S. Sarojam and S. J. Devaki, *ACS Sustain. Chem. Eng.*, 2016, **4**, 3535–3543.

12 D. J. Bozym, S. Korkut, M. A. Pope and I. A. Aksay, *ACS Sustain. Chem. Eng.*, 2016, **4**, 7167–7174.

13 P. Iamprasertkun, A. Krittayavathananon and M. Sawangphruk, *Carbon N. Y.*, 2016, **102**, 455–461.

14 S. K. Simotwo, P. R. Chinnam, S. L. Wunder and V. Kalra, *ACS Appl. Mater. Interfaces*, 2017, **9**, 33749–33757.

15 X. Wang, Y. Li, F. Lou, M. E. Melandsø Buan, E. Sheridan and D. Chen, *RSC Adv.*, 2017, **7**, 23859–23865.

16 R. Thangavel, A. G. Kannan, R. Ponraj, V. Thangavel, D. W. Kim and Y. S. Lee, *J. Power Sources*, 2018, **383**, 102–109.

17 J. Sun, J. Niu, M. Liu, J. Ji, M. Dou and F. Wang, *Appl. Surf. Sci.*, 2018, **427**, 807–813.

18 L. Wang, G. Mu, C. Tian, L. Sun, W. Zhou, P. Yu, J. Yin and H. Fu, *ChemSusChem*, 2013, **6**, 880–889.

19 X. He, P. Ling, J. Qiu, M. Yu, X. Zhang, C. Yu and M. Zheng, *J. Power Sources*,

2013, **240**, 109–113.

20 A. M. Navarro-Suárez, J. Carretero-González, V. Roddatis, E. Goikolea, J. Ségalini, E. Redondo, T. Rojo and R. Mysyk, *RSC Adv.*, 2014, **4**, 48336–48343.

21 B. Krüner, J. Lee, N. Jäckel, A. Tolosa and V. Presser, *ACS Appl. Mater. Interfaces*, 2016, **8**, 9104–9115.

22 D. Xu, X. N. Sun, W. Hu and X. Y. Chen, *J. Power Sources*, 2017, **357**, 107–116.

23 L. X. Cheng, Y. Q. Zhu, X. Y. Chen and Z. J. Zhang, *Ind. Eng. Chem. Res.*, 2015, **54**, 9948–9955.

24 X. N. Sun, W. Hu, D. Xu, X. Y. Chen and P. Cui, *Ind. Eng. Chem. Res.*, 2017, **56**, 2433–2443.

25 L. Ren, G. Zhang, Z. Yan, L. Kang, H. Xu, F. Shi, Z. Lei and Z. H. Liu, *Electrochim. Acta*, 2017, **231**, 705–712.

26 A. Singh and A. Chandra, *Sci. Rep.*, 2016, **6**, 1–13.

27 Fan, L. Q.; Zhong, J.; Zhang, C. Y.; Wu, J. H.; Wei, Y. L. *Int. J. Hydrogen Energy* 2016, ***41***, 5725–5732.

28 Senthilkumar, S. T.; Selvan, R. K.; Ponpandian, N.; Melo, J. S.; Lee, Y. S. *J. Mater. Chem. A* 2013, ***1***, 7913–7919.

*****